Identification and characterization of *Sr13*, a tetraploid wheat gene that confers resistance to the Ug99 stem rust race group

Wenjun Zhang[a,1], Shisheng Chen[a,1], Zewdie Abate[a], Jayaveeramuthu Nirmala[b], Matthew N. Rouse[b,c,2], and Jorge Dubcovsky[a,d,2]

[a]Department of Plant Sciences, University of California, Davis, CA 95616; [b]Department of Plant Pathology, University of Minnesota, St. Paul, MN 55108; [c]US Department of Agriculture-Agricultural Research Service, Cereal Disease Laboratory, University of Minnesota, St. Paul, MN 55108; and [d]Howard Hughes Medical Institute, Chevy Chase, MD 20815

Contributed by Jorge Dubcovsky, September 25, 2017 (sent for review April 24, 2017; reviewed by Paul Schulze-Lefert and Brian J. Staskawicz)

The *Puccinia graminis* f. sp. *tritici* (*Pgt*) Ug99 race group is virulent to most stem rust resistance genes currently deployed in wheat and poses a threat to global wheat production. The durum wheat (*Triticum turgidum* ssp. *durum*) gene *Sr13* confers resistance to Ug99 and other virulent races, and is more effective at high temperatures. Using map-based cloning, we delimited a candidate region including two linked genes encoding coiled-coil nucleotide-binding leucine-rich repeat proteins designated CNL3 and CNL13. Three independent truncation mutations identified in each of these genes demonstrated that only *CNL13* was required for Ug99 resistance. Transformation of an 8-kb genomic sequence including *CNL13* into the susceptible wheat variety Fielder was sufficient to confer resistance to Ug99, confirming that *CNL13* is *Sr13*. *CNL13* transcripts were slightly down-regulated 2–6 days after *Pgt* inoculation and were not affected by temperature. By contrast, six pathogenesis-related (*PR*) genes were up-regulated at high temperatures only when both *Sr13* and *Pgt* were present, suggesting that they may contribute to the high temperature resistance mechanism. We identified three *Sr13*-resistant haplotypes, which were present in one-third of cultivated emmer and durum wheats but absent in most tested common wheats (*Triticum aestivum*). These results suggest that *Sr13* can be used to improve Ug99 resistance in a large proportion of modern wheat cultivars. To accelerate its deployment, we developed a diagnostic marker for *Sr13*. The identification of *Sr13* expands the number of *Pgt*-resistance genes that can be incorporated into multigene transgenic cassettes to control this devastating disease.

durum wheat | stem rust | Ug99 | resistance genes | CC-NBS-LRR

Stem rust of wheat, caused by the fungus *Puccinia graminis* f. sp. *tritici* (*Pgt*), is a serious wheat disease that has historically caused large yield losses worldwide. An isolate of *Pgt* identified in Uganda in 1998 (known as Ug99) is virulent to multiple stem rust resistance genes including the widely deployed *Sr31* (1). This race was later designated TTKSK using the North American stem rust nomenclature system (2). As TTKSK spread through Africa and the Middle East, it gained new virulences to wheat cultivars carrying resistance genes *Sr24* (2), *Sr36* (3), *Sr9h* (4, 5), and *SrTmp* (6). The expansion of the Ug99 race group to 10 countries in Africa, Egypt, Yemen, and Iran (7, 8) has prompted the search for new sources of resistance. This search has been broadened to other virulent races outside the Ug99 race group, such as TKTTF that caused severe stem rust epidemics in southern Ethiopia since 2013 (9). The recent experience in Ethiopia emphasizes the need for resistance genes with broader resistance or for combinations of resistance genes that can confer a broader and more durable resistance.

Among more than 70 *Sr* resistance loci that have been cataloged and assigned official or temporary designations, roughly half of them are effective against the Ug99 race group (7). However, only two slow-rusting adult plant resistance genes and five all-stage resistance genes effective against Ug99 have been cloned so far, likely reflecting the difficulties imposed by the large and complex wheat genomes. The two slow-rusting genes include *Sr57*/*Lr34* and *Sr55*/*Lr67*, which encode a putative ABC transporter (10) and a hexose transporter (11), respectively. The five all-stage resistance genes identified so far include *Sr35* (12) and *Sr22* (13) from diploid wheat *Triticum monococcum* L.; *Sr33* (14) and *Sr45* (13) from diploid *Aegilops tauschii* Coss.; and *Sr50* from diploid rye (*Secale cereale* L.) (15). These five genes encode coiled-coil nucleotide-binding leucine-rich repeat (CC-NBS-LRR) proteins, hereafter designated as CC-NBS-LRR genes (NLRs). Chromosomes of *T. monococcum* and rye carrying these resistance genes recombine poorly with wheat chromosomes (16, 17), so the *Pairing homeologous 1* mutation (*ph1b*) is required to induce homeologous recombination to reduce the size of the introgressed chromosome segments. The chromosomes of *A. tauschii* recombine well with the polyploid wheat D genome chromosomes, although the frequencies of recombination are sometimes reduced in the most divergent accessions (18).

The transfer of resistance genes directly from the wheat primary gene pool minimizes the need for additional rounds of homeologous recombination in the *ph1b* background. One of

Significance

Wheat provides a substantial proportion of the calories and proteins consumed by humans, but further production increases are necessary to feed a growing human population. Reducing yield losses caused by pathogens can contribute to these increases. In this study, we report the identification of *Sr13*, a gene from pasta wheat that confers resistance to the new virulent races of the stem rust pathogen that appeared in Africa at the beginning of this century. We identified three different resistance forms of *Sr13* and developed a diagnostic marker to accelerate their deployment in wheat breeding programs. In addition, *Sr13* can be a useful component of transgenic cassettes including multiple resistance genes.

Author contributions: M.N.R. and J.D. designed research; W.Z., S.C., Z.A., J.N., and M.N.R. performed research; W.Z., S.C., J.N., M.N.R., and J.D. analyzed data; W.Z., S.C., M.N.R., and J.D. wrote the paper; and J.D. supervised the project.

Reviewers: P.S.-L., Max Planck Institute for Plant Breeding Research; and B.J.S., University of California, Berkeley.

The authors declare no conflict of interest.

Data deposition: The sequences reported in this paper have been deposited in the GenBank database (accession nos. KY825225–KY825235 and KY924305).

[1]W.Z. and S.C. contributed equally to this work.

[2]To whom correspondence may be addressed. Email: matthew.rouse@ars.usda.gov or jdubcovsky@ucdavis.edu.

This article contains supporting information online at www.pnas.org/lookup/suppl/doi:10.1073/pnas.1706277114/-/DCSupplemental.

these resistance genes, *Sr13*, was identified first in durum wheat [*Triticum turgidum* ssp. *durum* (Desf.) Husn.] and was then transferred to hexaploid wheat (Khapstein/9*LMPG) (19). The domesticated emmer wheat [*T. turgidum* ssp. *dicoccon* (Schrank ex Schüebler) Thell.] Khapli (20) and the tetraploid Ethiopian accession ST464 (21) were used as sources of *Sr13* in durum wheat. *Sr13* confers resistance to all races in the Ug99 group (typical infection types range from 2 to 2+) (22), but the resistant reaction is influenced by temperature and genetic background (23, 24).

Sr13 has been mapped on the distal region of chromosome arm 6AL (25), but the development of diagnostic molecular markers has been delayed likely due to the different germplasm sources used to transfer *Sr13* into modern cultivated wheats (20, 21, 25). The map-based cloning and characterization of the stem rust resistant gene *Sr13* reported in this study revealed the existence of three different resistant haplotypes with some differences in resistance profiles. All three haplotypes confer resistance to the Ug99 race group and to the virulent races TKTTF and TRTTF outside the Ug99 race group.

Results

Construction of Genetic and Physical Maps of the *Sr13* Region. *Sr13* was previously mapped on the distal region of the long arm of chromosome 6A of durum wheat within a ~1.2-cM interval flanked by markers *CD926040* and *barc104c* (25). In this study, we generated a larger mapping population (12,162 gametes) from the cross Kronos × Rusty and identified 45 recombination events between these two flanking markers, providing a better estimate of their genetic distance (0.4 cM). We generated additional markers in the region (*SI Appendix*, Table S1 and *Method S1*) and mapped *Sr13* completely linked to *EX24785*, within a 0.08-cM interval delimited by markers *CJ641478* and *CJ671993* (Fig. 1 *A* and *B*).

We screened the bacterial artificial chromosome (BAC) library of the *Sr13*-resistant durum wheat variety Langdon (26) with marker *EX24785* and identified BAC 156P14. Sequencing of this BAC revealed two NLR genes (*CNL1* and *CNL3*) and two 5′ or 3′ truncated NLR genes (*cnl2* and *cnl4*). We developed markers for these complete and truncated NLR genes and mapped *Sr13* within a 0.02-cM interval delimited by *cnl2* and *CJ641478* (Fig. 1*B*). We developed a physical map of this region including nine overlapping BACs (Fig. 1*C*, 955 kb) that were sequenced, annotated, and deposited in GenBank as accession no. KY924305.

The 858-kb region between flanking markers *cnl2* and *CJ641478* (Fig. 1*D*) included two complete NLR genes (*CNL3* and *CNL13*), one gene annotated as 12-oxophytodienoate reductase 1 (*OPR1*), and 10 5′- or 3′-truncated NLR genes (Fig. 1*D*). Among the three complete genes, we prioritized the two NLR genes, which encode proteins frequently associated with pathogen recognition and initiation of resistance responses in plants. The linked gene *OPR1*, which encodes an enzyme involved in the jasmonic acid biosynthesis pathway, was considered a less likely candidate.

Validation of *Sr13* Candidate Genes Using Ethyl Methanesulfonate Mutants. To determine if *CNL3* or *CNL13* were required for resistance to Ug99 (TTKSK), we selected three truncation mutations for each gene from the recently published database of sequenced ethyl methanesulfonate mutations in Kronos (27). The three mutations identified in *CNL3* (mutant lines T4-3715, T4-1065, and T4-403) were all predicted to generate premature stop codons (Fig. 2*A*) and to encode nonfunctional truncated proteins. Plants homozygous for each of the three *CNL3* mutations showed levels of resistance to TTKSK similar to those observed in the resistant Kronos control (Fig. 2*B*). Similar results were observed when the three *CNL3* mutants were inoculated with races TKTTF, JRCQC, and TRTTF (*SI Appendix*, Fig. S1), which suggests that *CNL3* is not *Sr13*.

By contrast, plants homozygous for *CNL13* mutations encoding premature stop codons (mutant lines T4-3102 and T4-771) or an altered donor splice site (mutant line T4-476; Fig. 2*A*) were highly susceptible to TTKSK, and showed average pustule sizes significantly larger ($P < 0.05$) than those in Kronos (Fig. 2*B*). Similar results were obtained when the homozygous *CNL13*

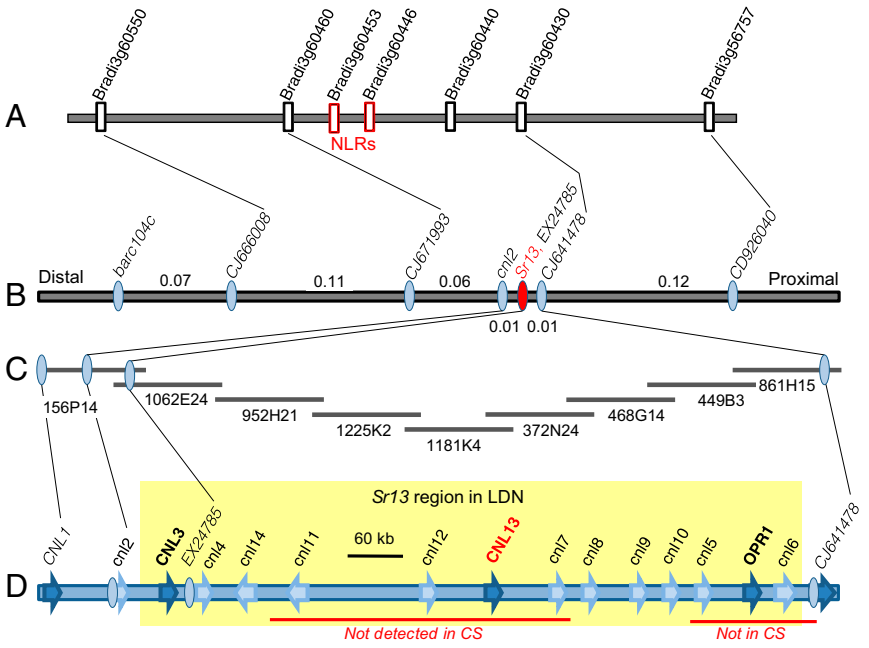

Fig. 1. Genetic and physical maps of *Sr13*. (*A*) *B. distachyon* chromosome 3 region colinear with the wheat *Sr13*-candidate region. Rectangles in red indicate NLR genes (likely nonfunctional since they carry frame-shift mutations and premature stop codons). (*B*) High-density genetic map of *Sr13* on chromosome arm 6AL. (*C*) Physical map of the *Sr13* region constructed with overlapping BACs from the *Sr13*-resistant durum wheat variety Langdon. (*D*) Diagrammatic representation of the annotated sequence of the *Sr13* region (GenBank accession no. KY924305). Genes are indicated by arrows (uppercase names indicate complete genes and lowercase names 5′ or 3′ truncated genes). Red lines below this graph indicate regions where no CS orthologs were found.

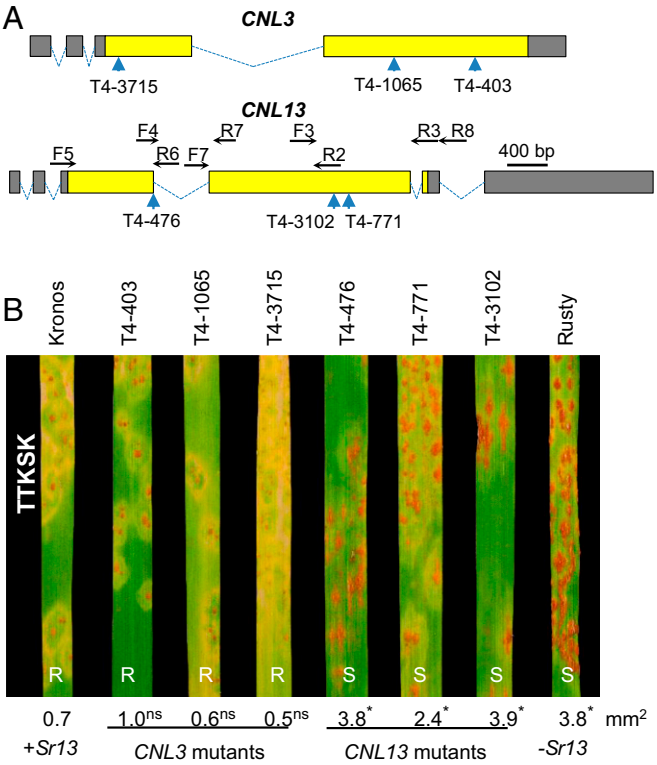

Fig. 2. *Sr13* mutants. (*A*) Schematic representation of NLR candidate genes *CNL3* and *CNL13*. Dotted lines indicate introns, yellow rectangles coding exons, and gray rectangles 5′ and 3′ UTRs. The positions of the selected truncation mutations are indicated by blue arrows. Mutations in Kronos mutant lines T4-403, T4-1065, T4-3715, T4-771, and T4-3102 are expected to result in premature stop codons, whereas the mutation in mutant line T4-476 is expected to eliminate the donor splice site of the third intron. (*B*) *CNL3* and *CNL13* mutant lines inoculated with race TTKSK. Kronos is the *Sr13*-resistant control and Rusty is the susceptible control. *CNL3* mutants are all resistant, whereas *CNL13* mutants are all susceptible to TTKSK (Ug99). Numbers below the leaves are average pustule sizes ($n = 3$). Superscripts indicate significance of the differences with Kronos using Dunnett's test (ns, not significantly larger than Kronos, $*P < 0.05$). Results for races TKTTF, JRCQC, and TRTTF are presented in *SI Appendix*, Fig. S1.

mutants were inoculated with races TKTTF and JRCQC (*SI Appendix*, Fig. S1). However, the same mutants inoculated with race TRTTF were all resistant, suggesting that Kronos carries another resistance gene effective against this race. To test this hypothesis, we selected F_2 plants from the cross Kronos × Rusty (25) that were either homozygous for the resistant (three plants) or for the susceptible (nine plants) *CNL13* alleles. Inoculation of the F_3 progeny of these plants with races TTKSK and JRCQC showed a perfect cosegregation between the *CNL13* allele and the phenotype (*SI Appendix*, Fig. S2). However, when the same plants were inoculated with race TRTTF, we observed resistant plants among the progeny of F_2 plants homozygous for the susceptible *CNL13* allele (*SI Appendix*, Fig. S2). This result confirmed the presence of a second TRTTF resistance gene in Kronos.

To characterize better the role of the *CNL13* LRR domain, we inoculated four additional lines carrying mutations in this region with *Pgt* race TTKSK. Mutations L757F (T4-3913), S730F (T4-4581), and D704N (T4-2561) had no effect on resistance to TTKSK, whereas mutation A717V (T4-4367) resulted in fully susceptible plants. This suggests that this LRR amino acid is important for TTKSK resistance (*SI Appendix*, Fig. S3). Taken together, these results demonstrated that *CNL13* is required for the *Sr13*-mediated resistance to races TTKSK, TKTTF, and JRCQC.

Validation of *Sr13* Using Transgenic Complementation. To test if *CNL13* was also sufficient to confer resistance to these races, we performed a transgenic complementation experiment using a complete genomic copy of *CNL13*. First, we identified the transcriptional start of the *CNL13* gene using 5′ rapid amplification of cDNA end (RACE, see *Materials and Methods*). The end of the transcript was determined from a previous Kronos transcriptome (27). Comparing Kronos *CNL13* transcripts with the corresponding genomic sequences revealed the presence of five introns, two of them in the 5′ untranslated region (UTR) and one in the 3′ UTR (Fig. 2*A*). The coding region, which starts in the third exon and ends in the fifth exon, extends for 2,847 bp (including the stop codon and excluding introns) and encodes a protein of 948 aa. The 538-bp 5′ untranslated region (UTR) included two introns, whereas the 2,187-bp 3′ UTR included a single intron (Fig. 2*A*, GenBank accession no. KY924305).

We cloned an 8,055-bp genomic fragment encompassing the complete transcribed region and transformed this construct into the Ug99-susceptible hexaploid common wheat variety Fielder. We obtained four independent transgenic events (T_0), which were confirmed with two independent sets of primers (*Materials and Methods*). Transgenic events T_1Sr13-1, T_1Sr13-3, T_1Sr13-4 showed a 3:1 transgene segregation ratio, suggesting the presence of a single copy of *CNL13*. This result was confirmed using a TaqMan Copy Number Assay (*SI Appendix*, Table S2). By contrast, we detected the presence of the transgene in all 80 T_1 plants from family T_1Sr13-2, suggesting the presence of at least three *CNL13* copies. This estimate was also supported by the TaqMan Copy Number Assay (*SI Appendix*, Table S2).

The differences in the number of inserted *CNL13* copies in the different transgenic events were not reflected in the expression levels. *CNL13* transcript levels in T_1Sr13-1, T_1Sr13-2, and T_1Sr13-3 were similar to each other and significantly higher than in the susceptible control Fielder (Fig. 3*A*). Those differences were not significant for plants from the T_1Sr13-4 family (Fig. 3*A*). In addition to the transgenic *CNL13* transcripts, the qRT-PCR primers used in this study also amplified the susceptible *CNL13* allele present in Fielder (see Sr13 *Allelic Variation*). To separate both alleles, we performed a semiquantitative PCR assay using the restriction enzyme *Hha*I, which generated a 265-bp fragment for the susceptible allele and a 244-bp fragment for the transgenic resistant allele (Fig. 3*B*). The semiquantitative PCR study confirmed that the transcript levels of the *CNL13*-resistant allele were higher in T_1Sr13-1, T_1Sr13-2, and T_1Sr13-3 than in T_1Sr13-4 (Fig. 3*B*).

T_1 plants from transgenic families T_1Sr13-2 and T_1Sr13-3 were more resistant to TTKSK than the untransformed control Fielder and showed significantly smaller pustules ($P < 0.001$; Fig. 3*C*). T_2 plants from selected T_1 plants from the four transgenic events showed resistance to races TTKSK, TKTTF, and TRTTF, and all exhibited average pustule sizes significantly smaller than those in Fielder ($P < 0.01$; *SI Appendix*, Fig. S4). Inoculation of Fielder and transgenic plants with race JRCQC provided no useful information because Fielder was highly resistant to this race. These transgenic experiments demonstrated that *CNL13* is sufficient to confer resistance to races TTKSK, TKTTF, and TRTTF.

Taken together, the complementation results, the mutant analyses, and the high-density genetic and physical maps demonstrated that *CNL13* is *Sr13*.

Effect of Temperature on Pathogen Growth and Gene Expression.

Effect of temperature on Pgt resistance. *Sr13* showed higher levels of resistance to TTKSK when plants were grown at high temperature (25 °C day/22 °C night) than when grown at lower temperature (18 °C day/15 °C night). The tetraploid variety Kronos (*Sr13*) was more resistant than Rusty (no *Sr13*) at both high and low temperature regimes, but the hexaploid isogenic lines LMPG (no *Sr13*) and Khapstein/9*LMPG (=LMPG-*Sr13*) were both

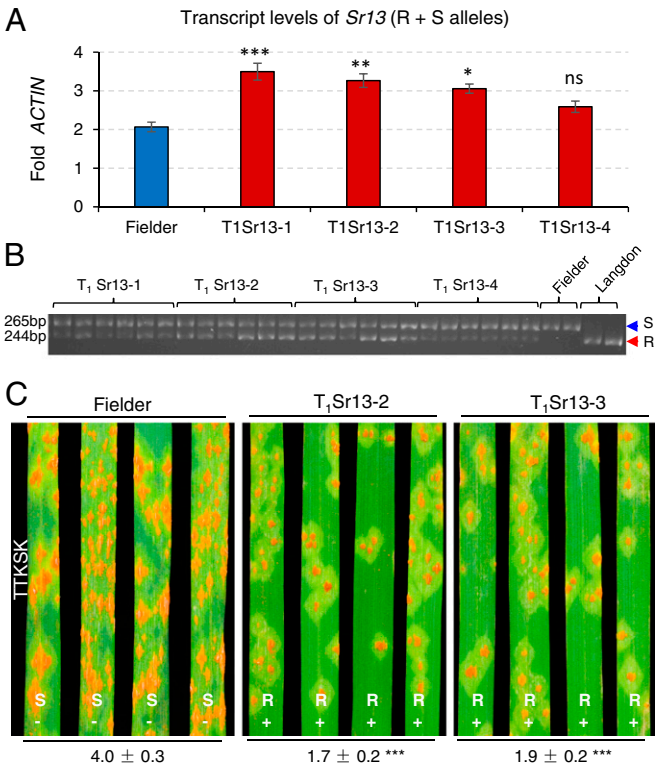

Fig. 3. Sr13 transgenic plants. (*A*) Transcript levels of *CNL13* in the susceptible control Fielder and in transgenic plants from four independent events (Fielder background). qRT-PCR primers amplify both the susceptible *CNL13* allele in Fielder (S1) and the resistant allele (R3) in the transgenic plants. Transcript levels are expressed as fold-*ACTIN* using the $2^{-\Delta CT}$ method. $*P < 0.05$, $**P < 0.01$, $***P < 0.001$, NS, not significant (Dunnett's test). (*B*) Semiquantitative PCR products from dCAPS marker Sr13F/R digested with restriction enzyme *Hha*I. The lower band corresponds to the transcript from the resistant allele (R = LDN) and the upper band to the transcript from the susceptible allele (S = Fielder). Six independent T_1 plants from every transgenic event were evaluated. (*C*) Reaction to *Pgt* race TTKSK (Ug99) in Fielder and transgenic families T_1Sr13-2 and T_1Sr13-3. R, Resistant; S, Susceptible; –, no resistant *CNL13* allele; +, resistant *CNL13* allele present. Numbers below leaves are average pustule sizes ($n = 8$). Superscripts indicate significance of the differences between Fielder and each of the transgenic families using Dunnett's test ($***P < 0.0001$). Results for the four transgenic families for races TTKSK, TKTTF, and TRTTF are presented in *SI Appendix*, Fig. S4.

susceptible at low temperature and only differed at high temperature (*SI Appendix*, Fig. S5).

These observations were confirmed in a three-way ANOVA for average pustule size determined 13 d after inoculation (dpi) in eight independent plants. This analysis showed highly significant ($P < 0.0001$) effects for genotype, temperature, ploidy level, and for the three possible two-way interactions (*SI Appendix*, Table S3). The interactions between genotype and temperature can be visualized in Fig. 4 *A*–*C*. These interactions were also significant for Fielder and its derived *Sr13* transgenic lines and for Kronos and its respective *sr13*-mutants (*SI Appendix*, Table S4).

We also quantified the differences in TTKSK growth at 5 dpi by measuring the ratio of fungal DNA relative to host DNA (Fig. 4 *D*–*F*) and average infection areas using microscopy and a fluorescent dye that stains the pathogen (Figs. 4 *G*–*I* and 5). Both methods showed highly significant ($P < 0.0001$) differences between genotypes and between temperatures. We also detected highly significant interactions between genotype and temperature (*SI Appendix*, Table S4) that reflect the larger differences between genotypes at high than at low temperature (Fig. 4). The differences in fungal infection area between LMPG and LMPG-*Sr13* were also validated with *Pgt* race BCCBC (isolate 09CA115-2; *SI Appendix*, Fig. S6).

Effect of temperature on Sr13 transcription profiles. Transcript levels of *Sr13* were similar at low and high temperature but were consistently lower in TTKSK inoculated than in mock-inoculated plants at the four sampling times (*SI Appendix*, Fig. S7). A three-way factorial ANOVA confirmed the absence of differences between temperatures ($P = 0.84$), and the significant differences between TTKSK inoculated and mock-inoculated plants ($P < 0.0001$) and among sampling times ($P < 0.0001$) (*SI Appendix*, Table S5). The consistency of the differences between inoculations across days and temperatures was reflected in nonsignificant interactions among these factors (*SI Appendix*, Table S5). Plants inoculated with TTKSK showed an 8.2% decrease in *Sr13* transcript levels relative to the mock-inoculated control. No significant differences were detected between the first and second dpi or between the fourth and sixth dpi. However, a 15% decrease in *CNL13* transcript levels was detected in a statistical contrast between the first two versus the last two time points ($P < 0.0001$). This decrease cannot be completely attributed to the pathogen, because an 11.5% decrease ($P = 0.006$) was also observed between the same time points for the mock-inoculated plants. However, the decrease was larger (18.7%) and more significant for the plants inoculated with TTKSK.

Effect of temperature on the transcript levels of pathogenesis-related genes. We first compared the effect of TTKSK inoculation with mock inoculation at the high temperature regime on the transcript levels of pathogenesis-related genes (*PR* genes) *PR1*, *PR2*, *PR3*, *PR4*, *PR5*, and *PR9* in different genotypes. These comparisons included resistant tetraploid Kronos versus susceptible *sr13*-mutant line T4-476 (Fig. 6), susceptible hexaploid LMPG versus its isogenic resistant line LMPG-*Sr13* (*SI Appendix*, Fig. S8) and susceptible hexaploid Fielder versus the *Sr13* transgenic line T_1Sr13-2 (*SI Appendix*, Fig. S9).

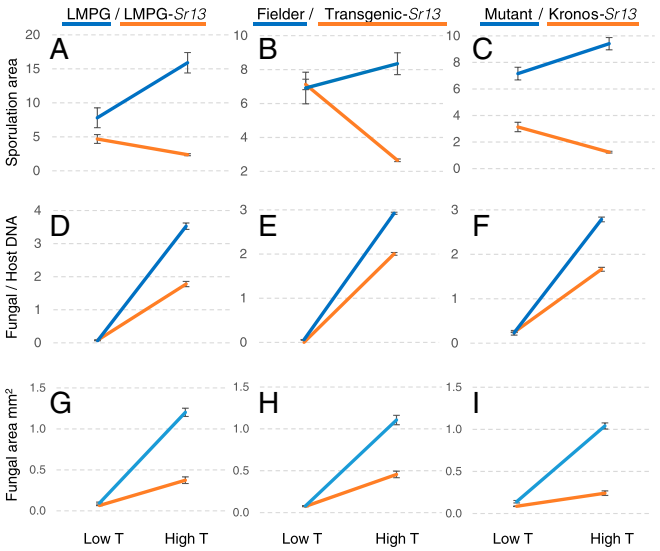

Fig. 4. Pathogen growth in different genotypes at different temperatures. Interaction graphs for pathogen growth at two temperatures (low = 18 °C day/15 °C night and high = 25 °C day/22 °C night) and in two genotypes (*Sr13* gene present or absent). Resistant genotypes are indicated in orange (LMPG-*Sr13*, transgenic-*Sr13*, and Kronos) and susceptible genotypes in blue (LMPG, Fielder, and Kronos *sr13*-mutant). Pathogen growth was estimated using average sporulation area 13 dpi (*A*–*C*), ratio between fungal and host DNA 5 dpi (*D*–*F*), and average size of individual fungal infection areas estimated by fluorescence microscopy 5 dpi (*G*–*I*). All plants were inoculated with TTKSK. Statistical analyses (including replication numbers) are detailed in *SI Appendix*, Table S4.

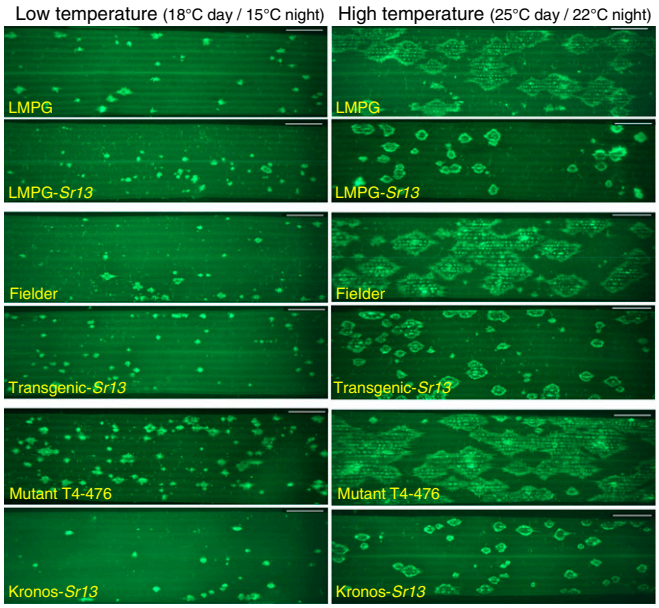

Fig. 5. Infection areas visualized by fluorescent staining. Visualization of TTKSK growth at different temperatures in resistant genotypes carrying *Sr13* (LMPG-*Sr13*, transgenic-*Sr13*, and Kronos) and in susceptible genotypes without *Sr13* (LMPG, Fielder, and Kronos *sr13*-mutant T4-476) 5 dpi. Infected leaves were cleared with KOH and stained with WGA-FITC.

Two-way ANOVAs showed highly significant differences between resistant and susceptible genotypes and between inoculations (*SI Appendix*, Table S6). We also detected highly significant interactions between genotype and inoculation that reflect the different *PR* profiles observed in resistant and susceptible genotypes. In the genotypes carrying *Sr13*, we observed a strong upregulation of all six *PR* genes after inoculation with TTKSK but not after mock inoculation (Fig. 6 and *SI Appendix*, Figs. S8 and S9). In the susceptible genotypes, we observed weaker responses that differed between genotypes. In the tetraploid *sr13*-mutants, all *PR* genes except *PR3* showed a slight but significant upregulation after inoculation with TTKSK relative to mock (Fig. 6). By contrast, in the susceptible hexaploid genotypes, most *PR* genes (except *PR5* and *PR9*) showed a significant downregulation after inoculation with TTKSK relative to mock (*SI Appendix*, Figs. S8 and S9 and Table S6). The opposite responses of susceptible and resistant hexaploid genotypes contributed to nonsignificant or less significant differences between inoculations for some *PR* genes (*SI Appendix*, Table S6).

We then studied the effect of different temperatures on the transcript levels of the *PR* genes (*SI Appendix*, Fig. S10). In Kronos plants inoculated with TTKSK or mock-inoculated at low and high temperatures, we observed highly significant ($P < 0.0001$) effects for temperature and inoculation (*SI Appendix*, Table S7). We also detected a highly significant interaction between temperature and inoculation because of the larger differences between TTKSK and mock-inoculated plants at high than at low temperatures (*SI Appendix*, Fig. S10). Similar results were observed for both sample collection times (4 and 6 dpi), although the overall transcript levels were higher ($P < 0.001$) 6 dpi than 4 dpi (except for *PR2*). In the mock-inoculated plants, we observed a small but significant increase ($P < 0.05$) in the transcript levels of all *PR* genes except *PR2* at low relative to high temperatures (*SI Appendix*, Fig. S10).

***Sr13* Allelic Variation.** Based on the sequence of Langdon BAC clone 1181K4 (Fig. 1; GenBank accession no. KY924305), we designed five pairs of gene-specific primers that amplify the complete coding and intron sequences of *CNL13* (*SI Appendix*, Table S1). Using these primers, we sequenced cultivars previously used to map *Sr13*, including four cultivars resistant to TTKSK (Kronos, Kofa, Medora, and Sceptre) and three cultivars susceptible against the same race (Rusty, UC1113, and Mindum) (25). We also sequenced the complete coding region of *CNL13* from the Ethiopian tetraploid landrace ST464 that carries *Sr13* (21) and from the hexaploid genetic stock Khapstein/9*LMPG that defines the *Sr13* gene name. As negative controls, we included the susceptible hexaploid lines LMPG, Fielder, and McNeal.

Among these lines, we found 10 DNA polymorphisms in the LRR region and two outside this region (*SI Appendix*, Fig. S11). We found three different haplotypes associated with resistance to TTKSK, which were designated R1 (Kronos and Khapstein/9*LMPG, KY825225), R2 (Kofa, Medora, and Sceptre, KY825226), and R3 (Langdon and ST464, KY924305). R2 and R3 differed from each other by two single nucleotide polymorphisms (SNPs), and both differed from R1 by three SNPs (*SI Appendix*, Fig. S11). We also identified four different haplotypes associated with susceptibility to TTKSK, which were designated S1 (Fielder, KY825227), S2 (UC1113, KY825228), S3 (LMPG, KY825229), and S4 (Rusty, Mindum, and McNeal). In the last three accessions, we failed to amplify any PCR product, which suggests that *CNL13* is deleted in these lines (*SI Appendix*, Fig. S11).

Since most *CNL13* polymorphisms were found in the LRR domain, we characterized the natural variation in this region in multiple accessions of *T. urartu* (74), *T. turgidum* ssp. *dicoccoides* (Koern. ex Asch. & Graebn.) Thell (50), *T. turgidum* ssp. *dicoccon* (90), *T. turgidum* ssp. *durum* (54), and *T. aestivum* (48, including three in which *Sr13* was introgressed from *T. turgidum* ssp. *dicoccon* accession Khapli). No PCR product was obtained for 70 accessions of *T. urartu* (94.6%), 47 of *T. turgidum* ssp. *dicoccoides* (94%), 37 of *T. turgidum* ssp. *dicoccon* (41.1%), 10 of *T. turgidum* ssp. *durum* (18.5%), and 18 of *T. aestivum* (37.5%),

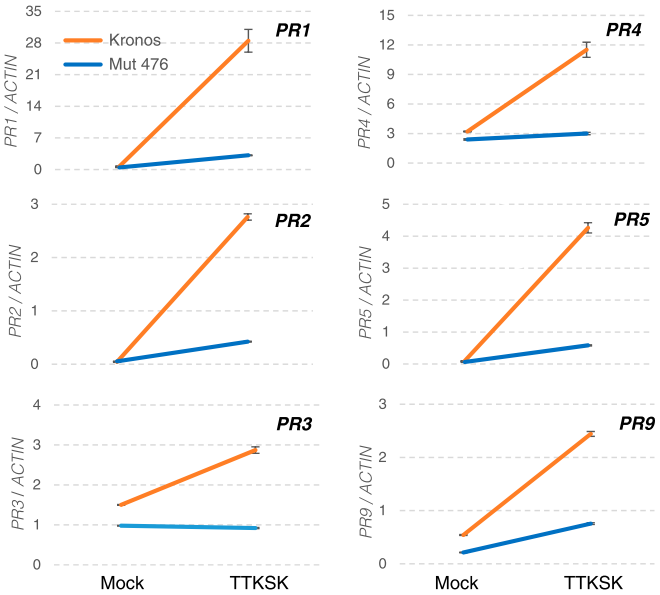

Fig. 6. Transcript levels of *PR* genes. Transcript levels of *PR* genes *PR1*, *PR2*, *PR3*, *PR4*, *PR5*, and *PR9* are presented in interaction graphs including two genotypes (Kronos *vs. sr13*-mutant T4-476) and two inoculation treatments (TTKSK vs. mock). Values relative to *ACTIN* endogenous control calculated using the ΔCT method. Error bars indicate SEMs. All interactions between genotype and inoculation were highly significant ($P < 0.001$). $n = 6$. Samples were collected 5 dpi. Statistical analyses are presented in *SI Appendix*, Table S6.

which suggests that *CNL13* is deleted in these accessions (*SI Appendix*, Table S8). The same DNAs were tested with primers for the positive control gene *RAR1* (*SI Appendix*, Table S1) to confirm that the lack of amplification was not due to degraded DNA. We evaluated these 182 lines with five pairs of primers (Fig. 2 and *SI Appendix*, Table S9). We were able to amplify a complete NLR gene in 20 accessions (98.2% identical to *Sr13*, with a premature stop codon at the end of exon 2 and a frame shift mutation in exon 3). For the rest, we amplified partial fragments from 41 accessions and failed to amplify any product from 121 accessions. Some of the amplified PCR fragments, including those from *T. urartu*, are likely from paralogs or nonfunctional copies based on their low identity to *Sr13* (*SI Appendix*, Table S9).

Among the 134 accessions for which we obtained PCR amplification products for the LRR region, 51 showed the 734R amino acid associated with resistance to TTKSK. Among these, we found 24 with the R1 haplotype, 21 with the R2 haplotype, and 6 with the R3 haplotype (*SI Appendix*, Table S8). To determine their resistance profiles, we inoculated accessions carrying each of these three haplotypes with races TTKSK, TKTTF, TRTTF, and JRCQC. Accessions carrying the R1 or R3 haplotypes showed resistance to all four races, but several of those carrying the R2 haplotype were susceptible to race JRCQC (*SI Appendix*, Fig. S12*A*). We confirmed that these differences were associated to *Sr13* by inoculating two *Sr13* homozygous resistant and two homozygous susceptible lines from the cross Kofa (R2) × UC1113 (S2) segregating for *Sr13.* Plants carrying the *CNL13* R2 allele were resistant to TTKSK and TRTTF but susceptible to JRCQC (*SI Appendix*, Fig. S12*B*). Based on this result, we designated the resistance allele associated with the R1 and R3 haplotypes as *Sr13a* and the one associated with the R2 haplotype as *Sr13b*.

Haplotypes R1, R2, and R3 were restricted in this survey to *T. turgidum* ssp. *dicoccon* and *T. turgidum* ssp. *durum* accessions (except for three *T. aestivum* genetic stocks in which *Sr13* was introgressed from Khapli). The only geographic region where we found all three resistant haplotypes was Ethiopia (in *T. turgidum* ssp. *dicoccon* accessions). Outside this region, we found two *T. turgidum* ssp. *dicoccon* accession carrying R2 (one in Spain and the other one in Saudi Arabia) and 11 carrying R1 [eight in India, one in Georgia, one in Russia, and one in Hungary (*SI Appendix*, Fig. S13 and Table S10)].

We obtained PCR products for the LRR region in *T. urartu* only for four (PI 428225, PI 428226, PI 428227, and PI 428251) of the 74 accessions tested. Sequencing of the PCR products revealed identical sequences among these four accessions that encoded a protein carrying the 734W amino acid associated with the susceptible alleles, but that were more divergent (93.8% identity) from the other 12 haplotypes, than those haplotypes were from each other (>98.6% identical, *SI Appendix*, Fig. S11). This result suggested that the *T. urartu* sequences correspond to a related paralog rather than to a *CNL13* ortholog. Previous studies have shown that these and other accessions of *T. urartu* are highly susceptible to TRTTF and, therefore, do not have *Sr13* (28). An identical sequence was found in a *T. turgidum* ssp. *dicoccoides* (PI 470955) collected close to the border between Syria and Turkey. The other two accessions of *T. turgidum* ssp. *dicoccoides* (collected in Israel) showed the *CNL13* S5 haplotype (*SI Appendix*, Table S10).

Among the tetraploid and hexaploid accessions for which we obtained *CNL13* LRR amplification products, we found the 734W amino acid associated with susceptibility in 78 accessions. These accessions included eight additional DNA polymorphisms, which defined six additional haplotypes. For each of these new haplotypes, we sequenced the complete gene for one accession (S5–S10, GenBank accession nos. KY825230–KY825235, *SI Appendix*, Fig. S11). In addition to these SNPs, haplotypes S8, S9, and S10 had insertions in the coding regions of 162, 17, and 3 bp, respectively. The 17-bp insertion in S9 altered the reading frame, modifying or eliminating the last 16 aa. A 48-bp insertion was found in the first intron of haplotypes S1 and S8. Inoculation of representative accessions for each of these new haplotypes with TTKSK revealed that at least one accessions per haplotype was susceptible to TTKSK (*SI Appendix*, Fig. S14), confirming that they were susceptible *CNL13* alleles. The geographic distribution of the different *CNL13* haplotypes is described in *SI Appendix*, Fig. S13 and Table S10.

The phylogenetic relationships among CNL1, CNL3, and CNL13 and their closest proteins in *T. aestivum*, *T. urartu*, *S. cereale*, *Hordeum vulgare*, and *Brachypodium distachyon* are described in *SI Appendix*, Fig. S15. These results suggest that the duplication of the three complete CNL proteins in this cluster originated before the wheat-rye divergence. Two of the three closest *B. distachyon* proteins (reconstructed by correcting frame shift mutations) were present in the CNL13 colinear region in the *B. distachyon* genome (Fig. 1).

An SNP Associated with *CNL13*-Resistant Haplotypes. A comparison between the *Sr13* susceptible and resistant haplotypes showed only one DNA polymorphism (T2200C, and its corresponding amino acid change W734R) that perfectly matched the differences between *Sr13* haplotypes susceptible and resistant to TTKSK (*SI Appendix*, Fig. S11). The amino acid change W to R is associated with a negative BLOSUM62 score (−3), which is indicative of a disruptive change for protein structure and function. To visualize the effect of this change on the LRR structure, we modeled the LRR domain of the R3 haplotype with both the 734R and 734W amino acids using Phyre 2 (29). The two structures revealed an α/β horseshoe fold typical of many LRR domains, but displayed large differences in the region flanking the W734R polymorphisms and in the two proximal β-sheets facing the interior side of the horseshoe fold (*SI Appendix*, Fig. S16).

The complete association detected so far between the T2200C SNP and resistance to TTKSK (*SI Appendix*, Table S8) suggests that a marker for this polymorphism would be a useful tool for selection of *Sr13* in wheat breeding programs. We designed a derived cleaved amplified polymorphic sequence (dCAPS) marker (*SI Appendix*, Table S1, primers *Sr13F*/*R*). Digestion of the amplification product with restriction enzyme *Hha*I yields a 244-bp band in accessions carrying the resistant haplotypes and a 265-bp band in accessions carrying the susceptible haplotypes (Fig. 3*B*). Lack of PCR amplification with these primers is indicative of the susceptible S4 allele.

We used this marker to clarify the relationship between *Sr13* and *Srdp2,* a gene first identified in *T. turgidum* subsp. *durum* accession PI 94701 (30). *Srdp2* was first proposed to be allelic to *Sr13* (23) and later suggested to be distinct from *Sr13* based on pathogenic variability studies (31). We found no PCR product for *Sr13* in the *Srdp2* donor lines PI 94701 and Golden Ball-derived W3504, supporting the hypothesis that *Srdp2* and *Sr13* are different genes.

Discussion

The *Sr13* Region. We mapped the *Sr13* gene to a ∼858-kb region including two complete NLR genes and 10 truncated NLR genes. NLR genes in both mammal and plant species tend to be organized in clusters of variable size, which provide a reservoir of genetic variation (32). The *Sr13* NLR cluster in Langdon (LDN, R3 haplotype) and Kronos (R1 haplotype) are almost identical. The two *CNL13* resistance alleles are 99.9% identical at the DNA level, and the sequences of all other complete and truncated NLR genes described in Fig. 1*D* are 100% identical between the two haplotypes. These results suggest a close evolutionary relationship between the regions, including the *CNL13* R1 and R3 haplotypes.

By contrast, the comparison of the 955-kb LDN sequence with the available genomic sequence of Chinese Spring (CS; haplotype S4) revealed limited conservation in this region. Only 8 of the 14 complete and truncated NLR genes were detected in CS (>98.5% DNA identity; Fig. 1*D*). The missing genes in the CS genome (including *CNL13*) define two large deleted regions of 368 kb and 50 kb, respectively (Fig. 1, red lines). Similar deletions seem to be present in the tetraploid Rusty (S4 haplotype), since primers for markers within these deletions did not yield PCR amplification products in this durum variety. We also identified four NLR-related sequences in CS and Rusty that were completely linked genetically to *CNL13*, which were not present in Kronos or Langdon. The extensive polymorphisms detected between the S4 and R3 haplotype in this region suggest rapid evolutionary changes within this NLR cluster in polyploid wheat, a characteristic that has been described before for other NLR clusters (33). The presence of large indels that differentiate Kronos and Rusty in this region explained the lack of recombination observed in the large region between *cnl2* and *CJ641478* (~858 kb; Fig. 1).

In the colinear region of *Brachypodium* chromosome 3 between *Bradi3g60460* (ortholog of wheat CJ671993) and *Bradi3g60430* (ortholog of wheat CJ641478), we identified two NLR annotated genes (*Bradi3g60446* and *Bradi3g60453*; Fig. 1), which encode proteins 75% and 66% similar (excluding indels larger than one amino acid) to wheat CNL13, respectively. This result suggests that this NLR cluster likely has a long evolutionary history that extends beyond the divergence between the *Triticum* and *Brachypodium* lineages (estimated 30–40 Mya; ref. 34). This conclusion is also consistent with the presence of large NLR clusters between CJ671993 and CJ641478 orthologs in CS chromosomes 6B (555 kb) and 6D (465 kb).

Identification and Initial Characterization of *CNL13*. The susceptibility to Ug99 of the four independent *CNL13* Kronos mutants and the resistance of the *CNL13* transgenic Fielder lines confirmed that this gene was both necessary and sufficient to confer resistance to Ug99 and, therefore, that *CNL13* is *Sr13*. We detected a single isoform of *CNL13* in our expression studies, which compared with the genomic sequence revealed the presence of complex 5′ and 3′ UTR including two and one intron, respectively. A complex UTR region with multiple introns was also described for the NLR gene *Sr35*, which also confers resistance to Ug99 (12). However, the role of these complex UTR regions is currently unknown. *CNL13* is expressed at relatively high levels in the leaves of Kronos (1- to 1.6-fold *ACTIN*) and is slightly down-regulated in the presence of the stem rust pathogen (8.2% decrease), suggesting that *Pgt* is not very effective in suppressing this gene.

Effect of Temperature on *Sr13*-Mediated Resistance and Gene Expression. Temperature is known to affect plant resistance to diseases, but the mechanisms are only partially understood (35). Known mechanisms include reduced steady-state resistance protein levels at high temperatures (36), temperature-sensing NB-LRR proteins (37), and salicylic acid (SA) regulation involving EDS1 and PAD4 (38, 39). In these studies, elevated growth temperature was associated with inhibition of the resistance response (35). Similar results have been observed for wheat *Pgt* resistance genes *Sr6*, *Sr10*, *Sr15*, and *Sr17*, which become more susceptible at increasing temperatures.

By contrast, *Sr13* was shown in previous studies (23, 24) and here to be more effective at high than at low temperature (Fig. 4 *A*–*C*). This observation was also supported by highly significant interactions between temperature and genotype in the three pairs of genotypes included in this study and in the three different methods used to estimate TTKSK growth (*SI Appendix*, Table S4). These consistent interactions indicate that the *Sr13*-mediated resistance is modulated by temperature. As wheat stem rust is often most problematic at relatively high temperatures (40), the temperature-sensitive *Sr13* resistance response could have been selected to optimize the balance between disease responsiveness and fitness.

At the early stages of the infection (5 dpi), the growth of the pathogen at low temperatures was slower for both the susceptible and resistant genotypes (Fig. 4 *D*–*I*). However, at the sporulation stage (13 dpi), the resistant genotypes showed reduced pathogen growth at high temperatures (Fig. 4 *A*–*C*), suggesting an active resistance mechanism of *Sr13*. This cannot be explained by differences in *Sr13* transcript levels because no significant differences were observed in its transcript levels between high and low temperatures.

By contrast, six *PR* genes showed a strong up-regulation at high but not at low temperature. We concluded that this up-regulation was dependent on the presence of the pathogen because we did not observe it in the mock-inoculated plants (*SI Appendix*, Fig. S10). This may reduce the fitness cost associated with *Sr13* in the absence of the pathogen. We also concluded that the up-regulation of the *PR* genes at high temperature was dependent on the presence of *Sr13* because it was not observed in the *sr13*-mutant (Fig. 6), or the LMPG (*SI Appendix*, Fig. S8) or Fielder (*SI Appendix*, Fig. S9) susceptible controls. Based on these results, we hypothesize that the strong and coordinated up-regulation of *PR* genes at high temperatures contributed to the higher levels of resistance to TTKSK conferred by *Sr13* under these conditions. This is consistent with the type of resistance conferred by *Sr13*. The *Sr13*-mediated resistance is not associated with the rapid cell death characteristic of a typical hypersensitive response, but rather with a slower growth of the pathogen at high temperatures in the presence of the resistance gene (Fig. 5). A chlorotic halo is observed around the *Pgt* pustules in the resistant reactions, which can eventually lead to cell death.

Finally, we also observed *Sr13*-independent mechanisms of *PR* gene regulation in wheat. The slower growth of the pathogen at low temperatures, together with the slight up-regulation of most *PR* genes at low temperatures in the susceptible genotype, can explain the reduced sporulation areas in the susceptible genotypes at low temperatures. In addition, in the susceptible hexaploid backgrounds, most of the *PR* genes were down-regulated by inoculation with TTKSK relative to mock. This observation suggests that *Pgt* has developed some mechanisms to down-regulate this defensive mechanism in hexaploid wheat. It would be interesting to investigate why this response was not observed in tetraploid Kronos.

Identification of Different CNL13 Haplotypes. Thirteen different haplotypes were detected in the *CNL13* LRR domain from 311 diploid, tetraploid, and hexaploid *Triticum* species (including S4 where the gene appears to be deleted). Evaluation of these different haplotypes with Ug99 revealed three resistant haplotypes (R1–R3) and 10 susceptible haplotypes (S1–S10). The additional haplotype found in *T. urartu* is likely from a close paralogous gene (*SI Appendix*, Fig. S15) and is not included in the haplotype analysis.

These haplotypes differed by 27 SNPs at the DNA level (18 in the LRR) and 25 aa at the protein level (16 in the LRR, *SI Appendix*, Fig. S11). The large ratio of nonsynonymous (25) to synonymous (2) substitutions suggests that the *CNL13* gene has been under positive selection, a hypothesis also supported by the Z test of positive selection as implemented in MEGA 6 (41). The number of nonsynonymous substitutions per nonsynonymous site (K_a) was significantly higher ($P < 0.05$) than the number of synonymous substitutions per synonymous site (Ks) for 47 of the 66 possible pairwise haplotype comparisons (*SI Appendix*, Table S11). Nonsynonymous substitutions were observed for 38 of the 66 pairwise comparisons (K_a/Ks = infinite), and for the other 28, the average K_a/Ks was 2.58 ± 0.17. This ratio is larger than one, which is the expected ratio under neutral selection. Positive selection has been reported in the LRR domains of multiple NLR genes (33). For *CNL13*, both the LRR and non-LRR region

appear to be under positive selection. However, the number of polymorphisms available in the non-LRR region is too low to make a confident conclusion.

The only amino acid change that was consistent with the susceptible and resistant haplotypes was a W to R change at position 734 within the LRR domain (*SI Appendix*, Fig. S11). The W734R mutation is associated with large changes in the predicted LRR structure (*SI Appendix*, Fig. S16). Based on this result, we hypothesize that the W734R polymorphism may play an important role in the detection of the pathogen. An additional induced mutation in the LRR domain (A717V) located only 17 amino acids apart from W734R was also associated with susceptibility, further supporting the hypothesis that this region of the LRR domain is critical for the *Sr13* resistance to TTKSK.

Evolution of Sr13. To trace the origin of the Ug99-resistant haplotypes, we analyzed the sequence variation in the *CNL13* LRR domain and the geographic distributions of the different haplotypes. A lack of amplification of the *CNL13* LRR domain (haplotype S4) was detected in 95% of the *T. urartu* accessions and 94% of the *T. turgidum* subsp. *dicoccoides* accessions included in this study. This result suggests that the S4 haplotype was likely transferred from *T. urartu* to the wild tetraploid wheats, although we cannot rule out independent deletion events.

The only *CNL13* allele amplified so far from *T. turgidum* subsp. *dicoccoides* was S5, detected in two accessions from Israel. The same allele was detected in five *T. turgidum* subsp. *dicoccon* accessions from Ethiopia, Iran, and Russia (*SI Appendix*, Fig. S13 and Table S10), suggesting a wide distribution. These results, together with the absence of differential SNPs in S5 (*SI Appendix*, Fig. S11, red) suggests that S5 may be similar to the ancestral *CNL13* haplotype.

Three indirect observations point to Ethiopia and neighboring countries as a likely region for the origin of the *CNL13*-resistant haplotypes. First, this is the only region where all three Ug99-resistant haplotypes were found, and that has the largest diversity of *CNL13* susceptible haplotypes (*SI Appendix*, Table S10). This diversity in *CNL13* may reflect a higher diversity in the pathogen population in this region. Preliminary results suggest that *Berberis holstii*, which is endemic to the highlands of East Africa, is a functional alternate host where *Pgt* can complete its sexual cycle (42). This may have contributed to the origin of the new virulences in the *Pgt* population (including the development of Ug99) and promoted the increased diversity in the *CNL13* gene in this region. Since a single SNP change can be used to diagnose the *CNL13*-resistant alleles, DNA extractions from ancient archeological samples of *T. turgidum* subsp. *dicoccon* from Ethiopia and India may provide interesting information on the origin and dispersion of the *CNL13*-resistant alleles. The presence of multiple *T. turgidum* subsp. *dicoccon* accessions from India carrying the R1-resistant haplotype are not surprising, given that connections between Ethiopia and India go back more than 2,000 y of recorded history.

So far, no *CNL13*-resistant haplotype has been detected in *T. turgidum* subsp. *dicoccoides*, suggesting that the haplotypes resistant to Ug99 may have originated in *T. turgidum* subsp. *dicoccon*. Selection likely contributed to the rapid increase in the frequency of the resistant alleles, found in ∼31% of the accessions from this subspecies (*SI Appendix*, Table S8). *Sr13* was then incorporated into modern durum cultivars derived from *T. turgidum* subsp. *dicoccon* accessions from Ethiopia (ST464) and India (Khapli) (20, 21). Among the 54 *T. turgidum* ssp. *durum* accessions analyzed so far, only ∼37% carried the *CNL13*-resistant alleles (*SI Appendix*, Table S8), which suggests that there is still a large proportion of durum accessions that can benefit from the incorporation of *Sr13*.

At the hexaploid level, the most frequent *CNL13* haplotypes were S1 (26 accessions) and S4 (18 accessions). The S3 haplotype was identified only in LMPG (*SI Appendix*, Table S8). The *CNL13* allele R1 was the only resistant allele found in hexaploid wheat, where it was transferred from *T. turgidum* subsp. *dicoccon* Khapli (*SI Appendix*, Table S8). However, since *Sr13* is present in several durum varieties, it is also expected to be present in synthetic wheat generated from *T. turgidum* subsp. *durum* × *A. tauschii* hybrids or in their derivatives (43). Indeed, we found *Sr13*-resistant alleles in three of the nine synthetic wheats we tested. The synthetics "ITMI Synthetic" and "CROC_1/*A. tauschii* (205)" showed the R3 haplotype of *Sr13*, and the synthetic "CETA/*A. tauschii* (327)" showed the R1 haplotype.

One additional explanation for the low frequency of the *Sr13* in common wheat is the lower level of resistance conferred by this gene in hexaploid compared with tetraploid genetic backgrounds (23, 24). The reasons for this reduction and the opportunities to improve the impact of this gene in common wheat are discussed in more detail below.

Utilization of *Sr13* in Breeding. The lower level of *Pgt* resistance conferred by *Sr13* when it is transferred from tetraploid to hexaploid wheat has been reported for other resistance genes transferred to hexaploid wheat from relatives of lower ploidy (44). This has been attributed to the presence of modifiers or inhibitors of the transferred resistance gene in hexaploid wheat. In few cases, such as the *Pm8* powdery mildew resistance gene, the reduced resistance of the transferred gene was found to vary among hexaploid backgrounds. For *Pm8*, it was possible to identify the chromosome region responsible for this reduction and to use this knowledge to enhance the effect of *Pm8* in hexaploid wheat (44). Similar studies may be useful to enhance the effectiveness of *Sr13* resistance to TTKSK in common wheat-breeding programs.

Sr13 was previously reported to be ineffective against races TRTTF and JRCQC, based on high infection reactions observed on hexaploid varieties Khapstein/9*LMPG and Combination VII (R1 haplotype) in greenhouse and field nurseries in Ethiopia (45). However, our results show that, under controlled environmental conditions, *Sr13a* is effective against races JRCQC, TRTTF, and TKTTF in both tetraploid and hexaploid wheat (*SI Appendix*, Figs. S2 and S4). This result is important, because TKTTF has caused severe yield losses in southern Ethiopia in the Ug99-resistant variety Digalu in 2013 and 2014 (9). For hexaploid wheat, a test of the effectiveness of *Sr13*-resistant haplotypes against JRCQC, TRTTF, and TKTTF in the field is still pending.

The resistance conferred by *Sr13* to different *Pgt* races suggests that this gene will be useful in tetraploid wheat breeding programs. For this purpose, the *Sr13a* allele is a better option than the *Sr13b* allele because of the additional resistance to race JRCQC. However, because of the rapid breakdown of *Sr* genes deployed singly, it would be better to combine *Sr13* with additional TTKSK resistance genes. The diagnostic marker *Sr13F/R* developed in this study can be used to accelerate the generation of these resistance gene pyramids in durum wheat breeding programs.

Once transgenic approaches gain a wider public acceptance, the cloning of *Sr13* will provide an additional resistance gene to include in transgenic cassettes combining multiple resistance genes. As more *Pgt* resistance genes become available, it would be important to combine genes that use different resistance mechanisms. The delayed pathogen growth and *PR* gene up-regulation associated with *Sr13* can complement the hypersensitive resistance mechanism associated with *Sr35* and other resistance gene (12). Transgenic cassettes of resistance genes have the advantage of introducing multiple resistance genes in a single step and in a single chromosome location. These multiple resistance loci can be traced with a single molecular marker and have a reduced risk of being disrupted by recombination, a problem frequently encountered when resistance gene pyramids are used by breeding programs based only on phenotypic selection.

In addition to the practical applications described above, the cloning of *Sr13* provides a tool to identify the *Pgt* effectors recognized by this gene and the proteins targeted by these effectors. A study of the downstream components of this resistance response can provide useful knowledge to develop more durable resistance strategies against this devastating pathogen.

Materials and Methods

Plant Materials. F_2 plants (6,081) from the cross of Kronos × Rusty were used to generate the *Sr13* high-density genetic map. A collection of 74 accessions of *T. urartu*, 50 of *T. turgidum* ssp. *dicoccoides*, 90 of *T. turgidum* ssp. *dicoccon*, 54 of *T. turgidum* ssp. *durum*, and 48 of *T. aestivum* was used to study the taxonomic and geographic distribution of the *Sr13* alleles. These accessions included the original source of *Sr13* (*T. turgidum* ssp. *dicoccon* Khapli), seven *T. turgidum* ssp. *durum* lines used as parents in *Sr13* mapping populations (Kronos, Medora, Sceptre, Kofa, Rusty, Mindum, UC1113) (25), and three hexaploid accessions with *Sr13* introgressions from Khapli (Khapstein/9*LMPG, W2691Sr13, and Combination VII). Seeds of the mutants used for validation were obtained from the Kronos sequenced EMS induced mutant population (27).

Stem Rust Assays. We tested the efficacy of *Sr13* resistance against *Pgt* races that caused epidemics in Kenya and/or Ethiopia [TTKSK (Ug99), TKTTF] in addition to other virulent races that were previously reported as virulent to *Sr13* (TRTTF, JRCQC). Race TKTTF, originally detected in Turkey in the 1990s, is currently distributed throughout Europe, West Asia, North Africa, and East Africa (8, 10). TRTTF and the closely related RRTTF race were first detected in Iran in 1997 and have been found later in Ethiopia, Yemen, and Pakistan (8, 39). JRCQC has been detected in Ethiopia recently (39) and as early as 1987 (31). Seedling resistance evaluations were performed at the US Department of Agriculture-Agricultural Research Service (USDA-ARS) Cereal Disease Laboratory using multiple *Puccinia graminis* f. sp. *tritici* races [TTKSK (Ug99) isolate 04KEN156/04, TRTTF isolate 06YEM34-1, JRCQC isolate 09ETH08-3, and TKTTF isolate 13ETH18-1].

Procedures for inoculation, incubation, and scoring disease reactions were reported previously (28) except that seedling assays were incubated in growth chambers maintained at 25 °C day/22 °C night after inoculation unless otherwise described. The effectiveness of *Sr13* in tetraploid and hexaploid wheat under two different temperature regimes (18 °C day/15 °C night and 25 °C day/22 °C night) was also evaluated at the USDA-ARS Cereal Disease Laboratory.

Marker Development and BAC Library Screening and Sequencing. The initial markers flanking *Sr13* were obtained from previous genetic maps (25). New genome-specific primers were developed from wheat genes orthologous to those located in the colinear region in *Brachypodium*. Additional markers were developed from NLR genes in the CS 6AL arm sequence and, as they became available, from the BACs of *T. turgidum* subsp. *durum* cultivar Langdon (26) used in the construction of the physical map. The physical map was assembled by chromosome walking, starting from the closest proximal marker *CJ641478* and from the completely linked marker *EX24785* in both directions.

DNAs were extracted from selected BACs using a large-construct kit (Qiagen) and sequenced with Illumina at the University of California (UC) Davis Genomic Center. Sequences were assembled using Galaxy (46), and gaps were filled by Sanger sequencing. Based on the BAC sequence, we designed additional genomic specific primers to rescreen the BAC library for new clones. The process was repeated until markers flanking *Sr13* in both directions were identified.

Sequencing Annotation. First, we identified and annotated repetitive elements using the Triticeae Repeat Sequence Database (https://wheat.pw.usda.gov/ITMI/Repeats/blastrepeats3.html). Host duplications flanking the repetitive elements were manually curated. The nonrepetitive sequences were then annotated using a combination of BLASTN searches against wheat EST collections and the TIGR Wheat Genome Database (blast.jcvi.org/euk-blast/index.cgi?project=tae1). We also used gene models generated by comparison of our genomic region with diploid and tetraploid wheat transcriptomes (wheat.pw.usda.gov/GG2/WheatTranscriptome/). Additional BLASTX searches were performed against the nonredundant GenBank database of plant proteins. The annotated sequences of the 955-kb physical map (including three gaps) and of the different *CNL13* haplotypes were submitted to GenBank using Sequin.

5′ RACE. To determine the transcriptional start of the *CNL13* gene, we used 5′ RACE. High quality total RNA was extracted from the resistant parent Kronos, and the FirstChoice RLM-RACE Kit (Invitrogen) was used to perform the RACE reactions as described before (12). Briefly, primers developed at the 5′ coding region of *CNL13* were used as the gene-specific primers for nested PCRs (*SI Appendix*, Table S1). The TA cloning kit (Invitrogen) was used to clone the PCR products from the 5′ RACE reactions, and selected positive clones were sequenced using the Sanger method.

Effect of Temperature and Genotype on Pathogen Growth. Seedlings of different genotypes with and without *Sr13* were grown in a greenhouse and at the three-leaf stage were transferred to growth chambers at two different temperature regimes (low temperature:18 °C day/15 °C night and high temperature: 25 °C day/22 °C night). Half of the plants were inoculated with *Pgt* race TTKSK, and the other half were mock-inoculated. All plants were grown under a long day photoperiod (16 h light and 8 h dark) with a light intensity of ~500 $\mu M \cdot m^{-2} \cdot s^{-1}$ and a humidity of 95%.

Pathogen growth was estimated by three different methods. The amount of fungal DNA relative to host DNA and the average fungal infection area (visualized by fluorescence) were determined 5 dpi, whereas the average pustule size was determined 13 dpi. Relative DNA amount was determined as described before (12). Average infection area was determined in infected leaves cleared with KOH (37 °C, 12 h) and stained with WGA-FITC (L4895-10MG; Sigma-Aldrich). Images were obtained with a Zeiss Discovery V20 fluorescent dissecting scopes, and average fluorescent area per leaf was estimated from 20 individual infection sites. Average sporulation area was determined from images of infected leaves using ASSES (version 2) image analysis software for plant disease quantification from the American Phytopathology Society (47). In each leaf, all sporulation areas were measured in two nonoverlapping regions of 60 mm^2.

Effect of Temperature and Pathogen Inoculation on *Sr13* and *PR* Genes Transcript Levels. Total RNA was extracted using Spectrum Plant Total RNA Kit (Sigma-Aldrich). First-strand cDNA was synthesized from 1 μg of total RNA using a High-Capacity cDNA Reverse Transcription Kit (Applied Biosystems). qRT-PCR was carried out on an ABI 7500 Fast Real-Time PCR System (Applied Biosystems) using Fast SYBR GREEN Master Mix. Transcript levels were expressed as fold-*ACTIN* levels (the number of molecules in the target/the number of *ACTIN* molecules) using the $2^{-\Delta CT}$ method as described before (48). We calculated the significance of the differences in expression levels using factorial ANOVAs and the SAS program version 9.4.

To evaluate the effect of temperature and *Pgt* inoculation on *Sr13* transcript levels, we developed qRT-PCR primers Sr13RTF1R1 (*SI Appendix*, Table S1). The forward primer was designed in the third exon and the reverse primer in the junction between exons three and four to avoid amplification from genomic DNA. Primer efficiencies were estimated using five fourfold cDNA dilutions (1:1, 1:4, 1:16, 1:64, and 1:256), with each reaction carried out in triplicate. The qRT-PCR primers used in this study showed a single product in dissociation curves and its efficiency was higher than 95% (*SI Appendix*, Table S1). For each treatment, three samples from three different Kronos plants were collected at four time points: 1, 2, 4, and 6 dpi with TTKSK, always at the same time of the day.

We also characterized the expression of six pathogenesis-related (*PR*) genes (*PR1*-AJ007348, *PR2*-Y18212, *PR3*-AB029934, *PR4*-AJ006098, *PR5*-AF442967, and *PR9*-X56011) in two experiments. In the first experiment, we compared the expression of these genes in Kronos and the *sr13*-mutant T4-476 inoculated with TTKSK or mock-inoculated (both at high temperature). In the second experiment, we used only the variety Kronos and evaluated the plants 4 and 6 dpi with TTKSK or mock-inoculated under high and low temperature regimes. Data were transformed to restore normality of residuals in the factorial ANOVAs and was analyzed using SAS v. 9.4.

Transformation. We cloned a genomic fragment of 8,055 bp from Langdon BAC 1181K4 into a *Hind*III-HF/*Spe*I linearized binary vector pLC41Hm (49). This fragment included the complete coding region and introns (3,513 bp) plus 2,108 bp upstream of the start codon (including the 538 bp 5′ UTR) and 2,434 bp downstream of the stop codon (including the 2,187 bp 3′ UTR). DNA was extracted using the QIAGEN Large-Construct Kit (QIAGEN), and PCR amplifications were performed using Phusion High-Fidelity DNA Polymerase (New England BioLabs). The construct was introduced into the Ug99-susceptible hexaploid wheat variety Fielder via *Agrobacterium tumefaciens*-mediated transformation. To validate the presence of the transgene, we used two independent pairs of PCR primers. Primers HptmikiF/R amplify the hygromycin resistance gene present in the pLC41Hm binary vector and primers 6ACNL13F3/R3 (digested with enzyme *Fau*I) amplify a region of the *CNL13* LRR domain (*SI Appendix*, Table S1). To estimate the number of copies inserted in each of the transgenic events, we used a TaqMan Copy

Number Assay that includes *CONSTANS2* as the single copy control gene (50). These results were further validated using progeny tests of the T_1 plants.

Transcript levels in the transgenic plants were estimated with qRT-PCR primers Sr13RTF1R1 (*SI Appendix*, Table S1) using the $2^{-\Delta CT}$ method and *ACTIN* as an endogenous control (48). The significance of the differences in transcript levels between Fielder and the transgenic plants was estimated using the Dunnett's test as implemented in SAS 9.4. Because Fielder has a susceptible *CNL13* allele (S1) that is also amplified by the qRT-PCR primers, we complemented this test with a semiquantitative PCR test using primers Sr13F/R and restriction enzyme *Hha*I to distinguish the two alleles (*SI Appendix*, Table S1).

ACKNOWLEDGMENTS. We thank M. Padilla for excellent technical support; L. Epstein (UC Davis) for her help in the quantification of the sporulation size; S. Chao (USDA-ARS Fargo), J. Dvorak (UC Davis), and Y. Jin (USDA Cereal Disease Laboratory) for providing critical materials; the UC Davis genome center for the BAC sequencing; and UC Davis plant transformation facility for the wheat transformation. Work at J.D.'s laboratory was supported by the Howard Hughes Medical Institute and USDA Grant 2017-67007-25939 from the USDA National Institute of Food and Agriculture (NIFA). Work at M.N.R. laboratory was supported by USDA-ARS appropriated project 5062-21220-021-00-D, the USDA-ARS National Plant Disease Recovery System, and National Research Initiative Competitive Grant 2017-67007-25939 from the USDA NIFA.

1. Pretorius ZA, Singh RP, Wagoire WW, Payne TS (2000) Detection of virulence to wheat stem rust resistance gene *Sr31* in *Puccinia graminis* f. sp. *tritici* in Uganda. *Plant Dis* 84: 203.
2. Jin Y, et al. (2008) Detection of virulence to resistance gene *Sr24* within race TTKS of *Puccinia graminis* f. sp *tritici*. *Plant Dis* 92:923–926.
3. Jin Y, et al. (2009) Detection of virulence to resistance gene *Sr36* within the TTKS race lineage of *Puccinia graminis* f. sp *tritici*. *Plant Dis* 93:367–370.
4. Pretorius ZA, Szabo G, Boshoff WHP, Herselman L, Visser B (2012) First report of a new TTKSF race of wheat stem rust (*Puccinia graminis* f. sp. *tritici*) in South Africa and Zimbabwe. A. Pretorius. *Plant Dis* 96:590.
5. Rouse MN, et al. (2014) Characterization of *Sr9h*, a wheat stem rust resistance allele effective to Ug99. *Theor Appl Genet* 127:1681–1688.
6. Patpour M, et al. (2016) First report of the Ug99 race group of wheat stem rust, *Puccinia graminis* f. sp. *tritici*, in Egypt in 2014. *Plant Dis* 100:863.
7. Singh RP, et al. (2015) Emergence and spread of new races of wheat stem rust fungus: Continued threat to food security and prospects of genetic control. *Phytopathology* 105:872–884.
8. Fetch T, Zegeye T, Park RF, Hodson D, Wanyera R (2016) Detection of wheat stem rust races TTHSK and PTKTK in the Ug99 race group in Kenya in 2014. *Plant Dis* 100: 1495–1495.
9. Olivera P, et al. (2015) Phenotypic and genotypic characterization of race TKTTF of *Puccinia graminis* f. sp. *tritici* that caused a wheat stem rust epidemic in southern Ethiopia in 2013-14. *Phytopathology* 105:917–928.
10. Krattinger SG, et al. (2009) A putative ABC transporter confers durable resistance to multiple fungal pathogens in wheat. *Science* 323:1360–1363.
11. Moore JW, et al. (2015) A recently evolved hexose transporter variant confers resistance to multiple pathogens in wheat. *Nat Genet* 47:1494–1498.
12. Saintenac C, et al. (2013) Identification of wheat gene *Sr35* that confers resistance to Ug99 stem rust race group. *Science* 341:783–786.
13. Steuernagel B, et al. (2016) Rapid cloning of disease-resistance genes in plants using mutagenesis and sequence capture. *Nat Biotechnol* 34:652–655.
14. Periyannan S, et al. (2013) The gene *Sr33*, an ortholog of barley *Mla* genes, encodes resistance to wheat stem rust race Ug99. *Science* 341:786–788.
15. Mago R, et al. (2015) The wheat *Sr50* gene reveals rich diversity at a cereal disease resistance locus. *Nat Plants* 1:15186.
16. Dubcovsky J, Luo M, Dvorak J (1995) Differentiation between homoeologous chromosomes 1A of wheat and $1A^m$ of *Triticum monococcum* and its recognition by the wheat *Ph1* locus. *Proc Natl Acad Sci USA* 92:6645–6649.
17. Lukaszewski AJ (1995) Physical distribution of translocation breakpoints in homoeologous recombinants induced by the absence of the *Ph1* gene in wheat and triticale. *Theor Appl Genet* 90:714–719.
18. Yoshida T, et al. (2010) *Vrn-D4* is a vernalization gene located on the centromeric region of chromosome 5D in hexaploid wheat. *Theor Appl Genet* 120:543–552.
19. Knott DR (1990) Near-isogenic lines of wheat carrying genes for stem rust resistance. *Crop Sci* 30:901–905.
20. Knott DR (1962) The inheritance of rust resistance: IX. The inheritance of resistance to races 15B and 56 of stem rust in the wheat variety Khapstein. *Can J Plant Sci* 42: 415–419.
21. Klindworth DL, Miller JD, Jin Y, Xu SS (2007) Chromosomal locations of genes for stem rust resistance in monogenic lines derived from tetraploid wheat accession ST464. *Crop Sci* 47:1441–1450.
22. Jin Y, et al. (2007) Characterization of seedling infection types and adult plant infection responses of monogenic Sr gene lines to race TTKS of *Puccinia graminis* f. sp *tritici*. *Plant Dis* 91:1096–1099.
23. McIntosh RA, Wellings CR, Park RF (1995) *Wheat Rusts, an Atlas of Resistance Genes* (CSIRO, Melbourne). Available at https://www.globalrust.org/sites/default/files/wheat_rust_atlas_full.pdf. Accessed October 11, 2017.
24. Roelfs AP, Mcvey DV (1979) Low infection types produced by *Puccinia graminis* f. sp. *tritici* and wheat lines with designated genes for resistance. *Phytopathology* 69: 722–730.
25. Simons K, et al. (2011) Genetic mapping of stem rust resistance gene *Sr13* in tetraploid wheat (*Triticum turgidum* ssp. *durum* L.). *Theor Appl Genet* 122:649–658.
26. Cenci A, et al. (2003) Construction and characterization of a half million clone BAC library of durum wheat (*Triticum turgidum* ssp. *durum*). *Theor Appl Genet* 107: 931–939.
27. Krasileva KV, et al. (2017) Uncovering hidden variation in polyploid wheat. *Proc Natl Acad Sci USA* 114:E913–E921.
28. Rouse MN, Jin Y (2011) Stem rust resistance in A-genome diploid relatives of wheat. *Plant Dis* 95:941–944.
29. Kelley LA, Mezulis S, Yates CM, Wass MN, Sternberg MJE (2015) The Phyre2 web portal for protein modeling, prediction and analysis. *Nat Protoc* 10:845–858.
30. Rondon MR, Gough FJ, Williams ND (1966) Inheritance of stem rust resistance in *Triticum aestivum* ssp. *vulgare* Reliance and Pi 94701 of *Triticum durum*. *Crop Sci* 6: 177–179.
31. Huerta-Espino J (1992) Analysis of wheat leaf and stem rust virulence on a worldwide basis. PhD thesis (University of Minnesota, St. Paul).
32. Jacob F, Vernaldi S, Maekawa T (2013) Evolution and conservation of plant NLR functions. *Front Immunol* 4:297.
33. Michelmore RW, Christopoulou M, Caldwell KS (2013) Impacts of resistance gene genetics, function, and evolution on a durable future. *Annu Rev Phytopathol* 51: 291–319.
34. Bossolini E, Wicker T, Knobel PA, Keller B (2007) Comparison of orthologous loci from small grass genomes Brachypodium and rice: Implications for wheat genomics and grass genome annotation. *Plant J* 49:704–717.
35. Alcázar R, Parker JE (2011) The impact of temperature on balancing immune responsiveness and growth in Arabidopsis. *Trends Plant Sci* 16:666–675.
36. Bieri S, et al. (2004) RAR1 positively controls steady state levels of barley MLA resistance proteins and enables sufficient MLA6 accumulation for effective resistance. *Plant Cell* 16:3480–3495.
37. Zhu Y, Qian WQ, Hua J (2010) Temperature modulates plant defense responses through NB-LRR proteins. *PLoS Path* 6:e1000844.
38. Yang S, Hua J (2004) A haplotype-specific resistance gene regulated by BONZAI1 mediates temperature-dependent growth control in Arabidopsis. *Plant Cell* 16:1060–1071.
39. Wang Y, Bao Z, Zhu Y, Hua J (2009) Analysis of temperature modulation of plant defense against biotrophic microbes. *Mol Plant Microbe Interact* 22:498–506.
40. Roelfs AP, Singh RP, Saari EE (1992) *Rust Diseases of Wheat: Concepts and Methods of Disease Management* (CIMMYT, Mexico).
41. Tamura K, Stecher G, Peterson D, Filipski A, Kumar S (2013) MEGA6: Molecular evolutionary genetics analysis version 6.0. *Mol Biol Evol* 30:2725–2729.
42. Lim M, et al. (2015) *Berberis holstii is functional as an alternate host of Puccinia graminis* in Ethiopia. *2015 BGRI Workshop* (BGRI, Sydney). Available at https://www.globalrust.org/content/berberis-holstii-functional-alternate-host-puccinia-graminis-ethiopia. Accessed October 11, 2017.
43. Warburton ML, et al. (2006) Bringing wild relatives back into the family: Recovering genetic diversity in CIMMYT improved wheat germplasm. *Euphytica* 149:289–301.
44. McIntosh RA, et al. (2011) Rye-derived powdery mildew resistance gene *Pm8* in wheat is suppressed by the *Pm3* locus. *Theor Appl Genet* 123:359–367.
45. Olivera PD, et al. (2012) Races of *Puccinia graminis* f. sp. *tritici* with combined virulence to *Sr13* and *Sr9e* in a field stem rust screening nursery in Ethiopia. *Plant Dis* 96: 623–628.
46. Bankevich A, et al. (2012) SPAdes: A new genome assembly algorithm and its applications to single-cell sequencing. *J Comput Biol* 19:455–477.
47. Lamari L (2008) *ASSESS 2.0 Image Analysis Software for Plant Disease Quantification* (Am Phytopatholog Soc, St. Paul).
48. Pearce S, Vanzetti LS, Dubcovsky J (2013) Exogenous gibberellins induce wheat spike development under short days only in the presence of *VERNALIZATION1*. *Plant Physiol* 163:1433–1445.
49. Ishida Y, Hiei Y, Komari T (2015) High efficiency wheat transformation mediated by *Agrobacterium tumefaciens*. *Proceedings of the 12th International Wheat Genetics Symposium*, eds Ogihara Y, Takumi S, Handa H (Springer Japan KK, Tokyo), pp 167–173.
50. Díaz A, Zikhali M, Turner AS, Isaac P, Laurie DA (2012) Copy number variation affecting the *Photoperiod-B1* and *Vernalization-A1* genes is associated with altered flowering time in wheat (*Triticum aestivum*). *PLoS One* 7:e33234.